Available online at www.sciencedirect.com
ScienceDirect
Journal of Chromatography B, 859 (2007) 170–177
JOURNAL OF CHROMATOGRAPHY B
www.elsevier.com/locate/chromb

Evaluation of sphingolipids changes in brain tissues of rats with pentylenetetrazol-induced kindled seizures using MALDI-TOF-MS

Xiaoqiong Ma[a,1], Guangyi Liu[b,1], Shuang Wang[c], Zhong Chen[c], Maode Lai[a], Ziyang Liu[d], Jun Yang[e,*]

[a] *Department of Pathology and Pathophysiology, Zhejiang University School of Medicine, China*
[b] *Kidney Disease Center of the First Affiliated Hospital, Zhejiang University School of Medicine, China*
[c] *Department of Pharmacology, Zhejiang University School of Medicine, China*
[d] *Department of Chemistry, College of Science, Zhejiang University, China*
[e] *Department of Toxicology, Zhejiang University School of Public Health, 388 Yu-Hang-Tang Road, Hangzhou, Zhejiang 310058, China*

Received 28 July 2007; accepted 19 September 2007
Available online 10 October 2007

Abstract

Abnormal lipid metabolism has been implicated in the pathogenesis of many neural system diseases, including epilepsy. Pentylenetetrazol (PTZ)-induced kindling in rodents is considered a model of human absence epilepsy and myoclonic, generalized tonic-clonic seizure. In an effort to further understand the mechanism for PTZ-induced seizure, we analyzed crude lipids and sphingolipids in the cortex, hippocampus, and brain stem of normal and PTZ-rats using delayed extraction matrix-assisted laser desorption ionization time-of-flight mass spectrometry (DE MALDI-TOF-MS). It was found that phosphatidylcholines dominated the crude lipids in different tissues and there were no obvious differences in crude lipid profiles of different tissues between normal and PTZ-rats. However, ceramide, sphingomyelins, and ceramide-monohexoside were differently distributed in normal and PTZ-rats. Using the reference mass spectra method established in our laboratory, it was shown that sphingomyelins and ceramide-monohexoside levels were elevated in the brain tissues of PTZ-rats. Ceramide levels were found to be higher in brain stem than in cortex and hippocampus of normal rats, and PTZ caused a general decrease in ceramide levels. These data suggest that changes in sphingolipid metabolism contribute to PTZ-induced seizure.

Keywords: Sphingolipids; MALDI-TOF-MS; Epilepsy; Seizure

1. Introduction

Abnormal lipid metabolism has been implicated in the pathogenesis of a large number of diseases, especially neurological disorders, as the nervous system has the second highest concentration of lipids, exceeded only by adipose tissue. These include many neurological disorders such as bipolar disorders and schizophrenia, and neurodegenerative diseases such as Alzheimer's, Parkinson's and Niemann-Pick diseases [1,2]. As a major class of lipids and the building blocks of eukaryotic membranes, the importance of sphingolipids in many cellular functions, such as growth, proliferation, differentiation, and cell death, has been gradually recognized [3,4]. Defects in either the biosynthesis and degradation pathways of sphingolipids are also associated with many diseases exhibiting neurological symptoms, such as Tay-Sachs, Fabry, Sandhoff, Gaucher, Krabbe diseases, hereditary sensory neuropathy type 1 (HSN1), as well as an infantile-onset symptomatic epilepsy syndrome [5–7].

Because of the close relationship between lipids and diseases, considerable effort has been devoted to study the different lipid metabolism under health and disease conditions in recent years. However, only after the advent of "lipidomics", in which several individual lipid components can be analyzed simultaneously by mass spectrometry (MS), have vast amounts of information been generated regarding the various changes of lipids in different states of health [1,2,8,9]. In particular, as the focus of study turns to neural system, "neurolipidomics" has been

* Corresponding author. Tel.: +86 571 88208140; fax: +86 571 88208140.
E-mail address: gastate@zju.edu.cn (J. Yang).
[1] These two authors contributed equally to this work.

1570-0232/$ – see front matter © 2007 Elsevier B.V. All rights reserved.
doi:10.1016/j.jchromb.2007.09.027

coined [10,11]. Among the different mass spectrometry techniques, matrix-assisted laser desorption ionization time-of-flight (MALDI-TOF)-MS has been widely used in the determination and analysis of different classes of lipids in various tissues and disease states [12], such as phospholipids in mammalian lenses [13,14], polar phospholipids in normal and dry eye rabbit tears [15], lipids in rat brain [16–18], polysialogangliosides in skate brain [19], sphingolipids in vitreous bodies of a Gaucher disease patient [20] and sphingolipids in cardiac valves of a Fabry disease patient [21].

Our laboratory has also used delayed extraction (DE) MALDI-TOF-MS to analyze the involvement of sphingolipids in *N*-methyl-*N*′-nitro-*N*-nitrosoguanidine (MNNG) induced receptor clustering [22,23]. Although LC-ESI-MS/MS is coming into favor for lipid analysis [24–30], MALDI-TOF-MS remains a good choice for sphingolipid analysis thanks to its high sensitivity and rapid throughput [31].

Seizure is a symptom of abnormal brain function associated with epilepsy. Kindling has been accepted as an experimental animal model for analyzing epilepsy and epileptogenesis, and assessing the effectiveness of antiepileptic drugs. Pentylenetetrazol (PTZ) is a central nervous system excitant. It is generally known that PTZ-induced kindling creates proconflict and convulsant effects in rodents, for which reasons it is considered as an adequate model of human absence epilepsy and myoclonic, generalized tonic-clonic seizure, although the exact mechanisms for how PTZ-induced kindling remain elusive [32]. In addition, whether PTZ could affect sphingolipid metabolism is not clear. Therefore, in this study, using PTZ-induced seizures in rats ("PTZ-rats") as the model system, we investigated the changes of sphingolipids in brain tissues using MALDI-TOF-MS. Since cortex, hippocampus and brain stem of rats can be cleanly separated from other parts of brain, these tissues from normal and PTZ-rats were selected for our experiments.

2. Experimental

2.1. Animals

The use and handling of animals in this study were conducted following the regulations of the *Guide for the Care and Use of Laboratory Animals*, Zhejiang University. Animals used in this study were male Sprague–Dawley rats between 300 and 400 g (Experimental Animal Center, Zhejiang University), maintained in individual cages with a 12-h light:12-h dark cycle (light on from 8:00 to 20:00). Water was given *ad libitum*. To induce kindling, pentylenetetrazol, 35 mg/kg, was injected ip every 48 h [33]; the control group was injected with saline vehicle. After each PTZ treatment, rats were placed separately under glass funnels, and mortality as well as the appearance of clonic and tonic seizure was recorded during individual observation for 30 min. The seizure intensities were classified as follows: 0, no response; stage 1, ear and facial twitching; stage 2, convulsive waves through the body; stage 3, myoclonic jerks, rearing; stage 4, turning over onto one side position; stage 5, turning over onto back position, generalized tonic-clonic seizures. Fully kindled rats were usually observed in 3 weeks. When a rodent had a seizure score of 2 in 2 min and increased to score 4 in 10 min and maintained above score 2 for 2 h after three consecutive injections, it was defined as fully kindled.

2.2. Tissue sectioning

Seven fully kindled rats and the same number of controls were anesthetized by intraperitoneal injection of sodium pentobarbital (>65 mg/kg) and were decapitated upon cessation of respiration [17]. The brains were quickly removed from the skull, and cortex, hippocampus and brain stem were separated, weighed and stored at −70 °C.

2.3. Crude lipid extraction

Crude lipids were extracted according to the method described by Folch et al. [34] as following: frozen brain samples were chopped and homogenized in chloroform/methanol (2:1) and finally diluted to 20-times the volume of the original tissue sample volume using chloroform/methanol (2:1). The extract was then mixed thoroughly with 0.2 volume of water and the mixture was separated into two phases by centrifugation. The lower phase, which contained the crude lipids, was removed and used for further analysis.

2.4. Sphingolipid extraction

The extraction of sphingolipids was conducted as described before [22]. Briefly, 1 ml lipid-containing, lower phase, described above, was dried by vacuum centrifugation in a centrifugal evaporator (Speed-Vac, Thermo Savant, Holbrook, NY). Five hundred microliters of methanol containing 0.1 M NaOH was added to each tube at 55 °C for 1 h to hydrolyze glycerophospholipids. After neutralization with 100 μl methanol containing with 1 M HCl, 500 μl hexane, and one drop of water were added to each sample. The samples were then centrifuged again at 6500 rpm for 15 min, and the lower phase was dried in a centrifugal evaporator after the upper phase was removed. The residue was mixed with 0.8 ml theoretical lower phase (chloroform:methanol:water, 86:14:1, v/v/v) and 0.2 ml theoretical upper phase (chloroform:methanol:water, 3:48:47, v/v/v) for the Folch partition, and centrifuged at 6500 rpm for 15 min. The lower phase was evaporated in a centrifugal evaporator after removing the upper phase to discard the salt. The residue, considered the crude sphingolipid fraction, was stored at −70 °C to await MALDI-TOF-MS analysis.

2.5. DE MALDI-TOF-MS analysis

Each sample obtained from the above procedure was dissolved in 5 μl chloroform–methanol (v/v, 2:1), followed by the addition of 5 μl matrix solution (0.5 M 2,5-dihydroxybenzoic acid (2,5-DHB, Sigma) solution in ethylacetate containing 0.1% TFA) in a 0.5 ml Eppendorff tube. The tube was vortexed vigorously and then centrifuged in a microcentrifuge for 1 min. One microliter of mixture was directly spotted onto the sample plate

and rapidly dried under a moderate warm stream of air in order to remove the organic solvent within seconds.

All the samples were analyzed using a Voyager-DE STR MALDI-TOF mass spectrometer (ABI Applied Biosystem, Framingham, MA) with a 337 nm N_2 laser. The mass spectra of the samples were obtained in positive ion mode. Mass/charge ratios (*m/z*) were measured in the reflector/delayed extraction mode with an accelerating voltage of 20 kV, grid voltage of 67%, and delay time of 100 ns. C_6 ceramide (MW 397.63, Sigma) was used to calibrate the instrument. Crude lipid spectra were acquired using a mass range from *m/z* 500 to 2000. Sphingolipids spectra were acquired using a mass range from *m/z* 500 to 1000.

2.6. Establishment of reference mass spectrum and relative quantification

For analyzing sphingolipids, we established a "reference mass spectrum" (RMS) method to deal with the problem of inter-animal variation, as well as the problem associated with the poor quantification ability of MALDI-TOF-MS. The basic principle is that only those peaks presented in all seven mass spectra from the same group of rats were chosen and put in the RMS. By doing so, the interference of inter-animal variation could be minimized. Since it is difficult to quantify the amount of each sphingolipid species using MALDI-TOF-MS, a relative quantification method was also created by comparing the ratio of different sphingolipid species instead of the absolute amount of each species. It was found in all the mass spectra obtained, peak 753.6, which corresponds to $[SMd18:1C18:0 + Na]^+$, always had the relative intensity of 100%, meaning it is the highest peak in the mass spectra. Thus, the relative intensities of other peaks were calculated by comparing to peak 753.6. Then the mean and standard deviation of the relative intensity of each peak were computed from seven rats in either control or PTZ-rats. Combining these data, a final RMS was established for each brain section of normal and PTZ-rats. All the comparisons were then conducted using these RMS.

2.7. Statistical analysis

Statistical analysis was performed with Student's *t*-test. Data are presented as mean ± S.D. A probability level of $p < 0.05$ was considered significant.

3. Results

3.1. Crude lipid analysis of rat brain tissues

Crude lipids extracted from cortex, hippocampus and brain stem of normal and PTZ-rats were analyzed by MALDI-TOF-MS. The MS profiles of all these brain tissues were similar to each other, and no obvious differences were observed. Two classes of phospholipids, e.g., phosphatidylcholines (PC) and sphingomyelins (SM) were readily identified; and the specific PC and SM species were assigned based on previous publications [16–18]. Shown in Fig. 1 are representative mass spectra of crude lipids from the cortex of normal and PTZ-rats. It was found that *m/z* ions corresponding to PC comprised the main ions in the spectra. The dominant mass peaks corresponded to PC 32:0 and PC 34:1. In addition to the molecular ions $[M + H]^+$, the $[M + Na]^+$ and $[M + K]^+$ adducts of the PC 32:0, PC 34:1 and SM 18:0 species were also observed, respectively. The major ions and the corresponding PC or SM species in the mass spectra are listed in Table 1.

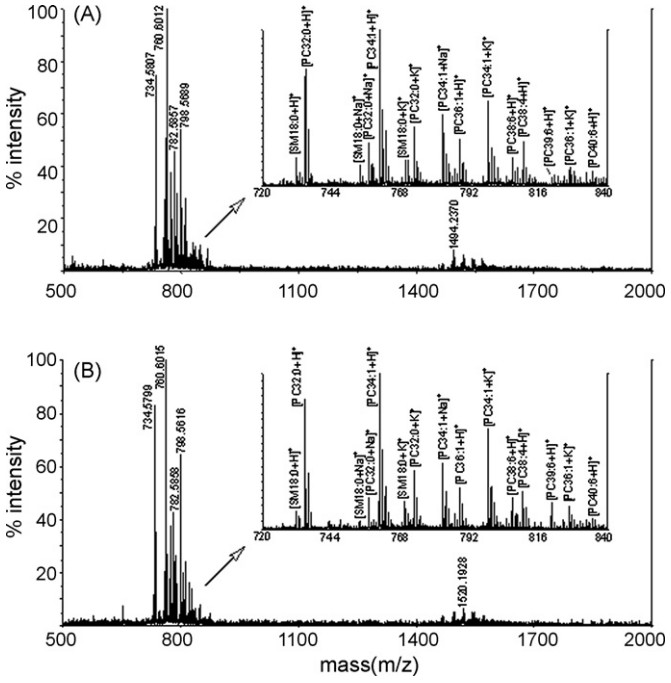

Fig. 1. Representative MALDI-TOF mass spectra of crude lipids in the cortex of normal and PTZ-rats. (A) Normal rats; (B) PTZ-rats.

Table 1
Phospholipid molecular species in crude lipids of rat brain tissues

Characteristic ions (*m/z*)	Molecular species
731.6	$[SM18:0 + H]^+$
734.6	$[PC32:0 + H]^+$
753.6	$[SM18:0 + Na]^+$
756.6	$[PC32:0 + Na]^+$
760.6	$[PC34:1 + H]^+$
769.6	$[SM18:0 + K]^+$
772.6	$[PC32:0 + K]^+$
782.6	$[PC34:1 + Na]^+$
788.6	$[PC36:1 + H]^+$
798.6	$[PC34:1 + K]^+$
806.6	$[PC38:6 + H]^+$
810.6	$[PC38:4 + H]^+$
820.6	$[PC39:6 + H]^+$
826.6	$[PC36:1 + K]^+$
834.6	$[PC40:6 + H]^+$
1468.2	$[2(PC32:0) + H]^+$
1494.2	$[(PC32:0) + (PC34:1) + H]^+$
1520.2	$[2(PC34:1) + H]^+$
1542.2	$[2(PC34:1) + Na]^+$
1566.2	$[(PC34:1) + (PC38:6) + H]^+$

SM: sphingomyelin; PC: phosphatidylcholine.

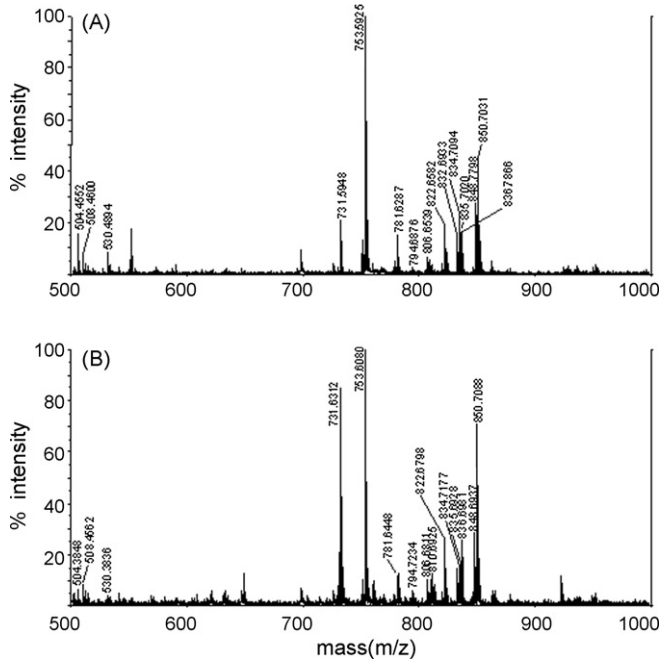

Fig. 2. Representative MALDI-TOF mass spectra of sphingolipids in the cortex of normal and PTZ-rats. (A) Normal rats; (B) PTZ-rats.

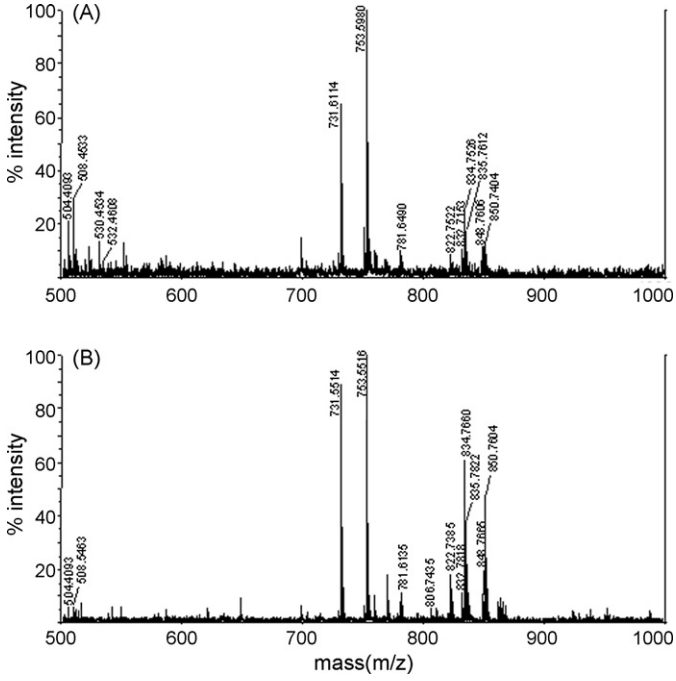

Fig. 3. Representative MALDI-TOF mass spectra of sphingolipids in the hippocampus of normal and PTZ-rats. (A) Normal rats; (B) PTZ-rats.

3.2. Sphingolipid analysis of rat brain tissues

Since PCs are the most abundant lipid in the crude lipid fraction of brain tissues, and since PCs and SMs can inhibit the detection of other phospholipids classes at similar concentrations in MALDI-TOF positive ion mode [35,36], it is necessary to remove PCs in order to measure accurately other phospholipids in rat brain extracts. Therefore, crude lipids were treated by mild alkalization, and sphingolipids were extracted and analyzed by MALDI-TOF-MS. Representative mass spectra of sphingolipids in the cortex, hippocampus, and brain stem of one normal and one PTZ-rat are shown in Figs. 2–4, respectively. And the RMS of sphingolipids in the brain tissues of normal and PTZ-rats was established, with 18 major peaks identified (Fig. 5). Three classes of sphingolipids, namely, ceramide (Cer), SM, and ceramide-monohexoside (CMH) were identified for these 18 peaks. After careful comparison to published data [37] and the sphingolipids database established by our laboratory (http://lipid.zju.edu.cn/), molecular ions $[M+Na]^+$ or $[M+H]^+$ for specific Cer, SM, and CMH species were assigned. The major ion assignments in the mass spectra are listed in Table 2.

Ceramide ions generally fall in the low mass regions of these spectra. It was found that the intensities of ions 504.4 (assigned to Cer[d18:1C12:0 + Na]$^+$), 508.5(Cer[d18:1C14:1 + H]$^+$), 530.5 (Cer[d18:1C14:1 + Na]$^+$) and 532.5(Cer[d18:1C14:0 + Na]$^+$) were higher in brain stem than in cortex and hippocampus of normal rats. But, the levels of all these ceramides decreased in PTZ-rats, with the most obvious decrease occurred in brain stem.

It was also observed that the relative intensity of *m/z* ions 731.6(SM[d18:1C18:0 + H]$^+$) increased in cortex and hippocampus but not in brain stem in PTZ-rats compared to controls. Similarly, the relative intensities of *m/z* ions 835.7(SM[d18:1C24:1 + Na]$^+$) was also increased in hippocampus of PTZ-rats; while the relative intensity of *m/z* ions 781.6(SM[d18:1C20:0 + Na]$^+$), 813.7(SM[d18:1C21h: 0 + Na]$^+$) and 835.7(SM[d18:1C24:1 + Na]$^+$) were increased in brain stem of PTZ-rats.

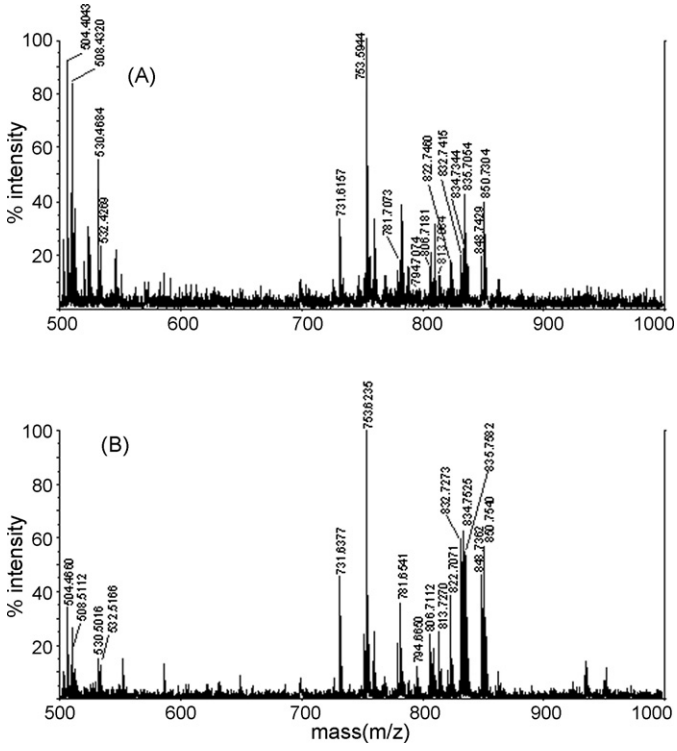

Fig. 4. Representative MALDI-TOF mass spectra of sphingolipids in the brain stem of normal and PTZ-rats. (A) Normal rats; (B) PTZ-rats.

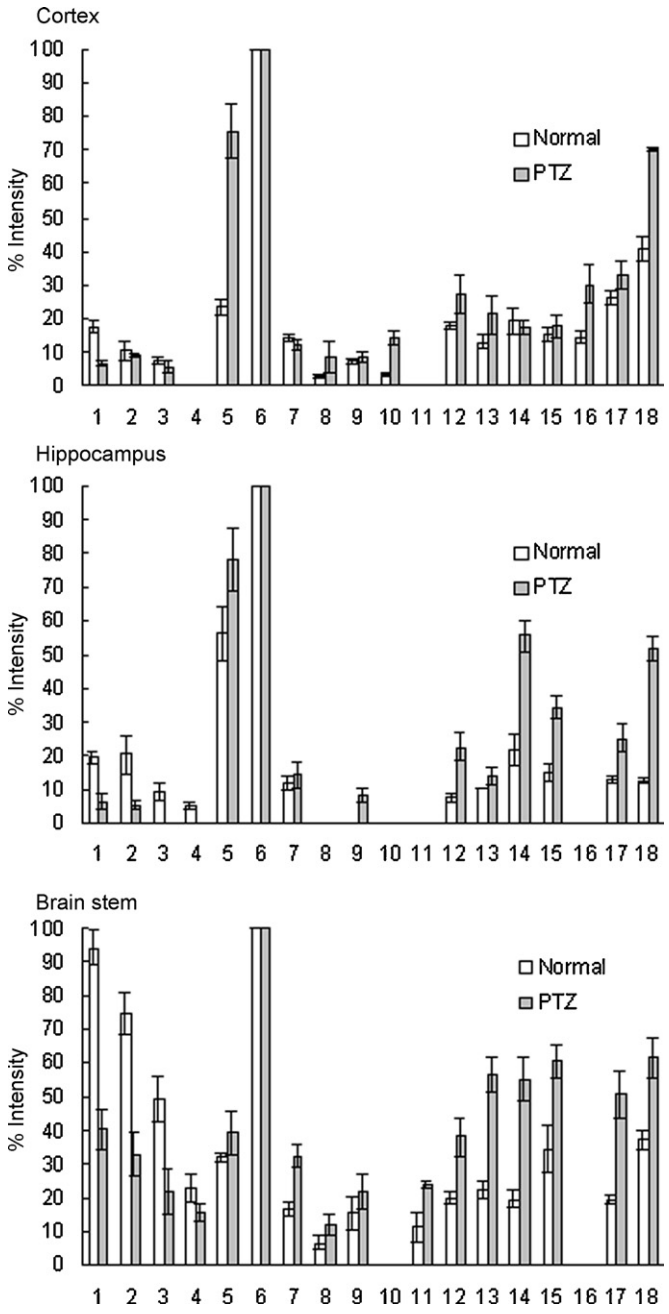

Fig. 5. Reference mass spectra of sphingolipids in the brain tissues of normal and PTZ-rats. Numbers 1–18 correspond to the index numbers in Table 2, representing the individual *m/z* ions.

For CMH species, it was found that the intensities of ions *m/z* 822.7(CMH[d18:1C22h:0 + Na]$^+$) and 850.7(CMH[d18:1C24h:0 + Na]$^+$) were increased in cortex, hippocampus and brain stem of PTZ-rats. In addition, the intensities of ion *m/z* 810.7(CMH[d18:1C24:1 + H]$^+$) and 836.7 (CMH[d18:0C24:0 + Na]$^+$) in cortex, ions *m/z* 806.7(CMH[d18:1C22:0 + Na]$^+$), 834.7(CMH[d18:1C24:0 + Na]$^+$), and 848.7 (CMH[d18:1C24h:0 + Na]$^+$) in hippocampus, ions *m/z*832.7 (CMH[d18:1C24:1 + Na]$^+$), 834.7(CMH[d18:1C24:0 + Na]$^+$), and 848.7(CMH[d18:1C24h:0 + Na]$^+$) in brain stem of PTZ-rats were also increased.

4. Discussion

Epilepsy is a common and heterogeneous neurological disorder with a number of subtypes arising from biochemical and molecular events that are not fully understood [38,39]. A variety of animal models have been developed to investigate epilepsy, such as kindling and status epilepticus, and many factors/events have been described during the process [32]. Recently, with the recognition of the importance of lipids in neurological diseases, the association between abnormal lipid metabolism and epilepsy has also been investigated. In particular, Simpson et al. reported that a homozygous, loss-of-function mutation of ganglioside GM3 synthase, the enzyme that synthesizes GM3 from lactosylceramide (LacCer), caused an infantile-onset symptomatic epilepsy syndrome, thus demonstrating the importance of sphingolipids in epilepsy [40].

However, systematic analysis of sphingolipids in epilepsy is still rare. In 2005, there was one report describing the change of sphingolipid levels in brains of patients suffering progressive epilepsy with mental retardation (EPRM). But the results were not clear cut, in that the sphingolipid levels were reduced in the brain of one progressive EPRM patient but increased in the brain of another, advanced EPRM patient [41]. Then in 2006, Guan et al. described the profiling of lipids, including ceramides, in hippocampal tissues during kainite treatment, which is commonly used to establish the status epilepticus model [42]. Therefore, in the present study, by applying a lipidomics paradigm, we systematically analyzed the sphingolipids in different rat brain tissues using the PTZ-kindling model.

To be able to analyze the complex mass spectra from a group of animals, we established a RMS method, like the "reference gel" in proteomic study. Since only those peaks presented in all animals of the same group were chosen, the individual variation should be minimized. However, by doing this procedure, some peaks that might reflect a real response to PTZ but only showed up in several animals, could be lost. In addition, MALDI-TOF-MS is not suitable for quantitative analysis, which posted another problem for drawing a RMS. Fortunately, it was found that peak 753.6 presented in all mass spectra and always had the highest intensity. Thus, peak 753.6 was used as the standard, and the relative intensity of all other peaks was calculated against it. This is based on the assumption that although the absolute value of each peak (the amount of corresponding shingolipid species) varies in each animal, the ratio between different peaks should be consistent among animals. Thus, the mean and standard deviation could be computed for each peak, and statistical analysis could also be conducted. Still, since we do not know whether peak 753.6 present in other type of samples, the application of this RMS method might be limited. However, in the future, if a universal internal standard could be defined or an external standard be added, RMS could be applied for different experiments, and comparison could be made among them.

It is not surprising that the dominant ions in crude lipids were PCs and SMs, as these two phospholipid species account for more than 50% of membrane phospholipids in eukaryotic organisms, with PC is by far the most abundant phospholipid [43]. As a structural component of membranes, PCs exhibited

Table 2
The average relative intensity of major sphingolipids in the cortex, hippocampus, and brain stem of normal and PTZ-rats

No.	Characteristic sphingolipid ions (*m*/*z*)	Cortex (mean ± S.D.)		Hippocampus (mean ± S.D.)		Brain stem (mean ± S.D.)	
		Normal	PTZ	Normal	PTZ	Normal	PTZ
1	504.4Cer[d18:1C12:0 + Na]$^+$	17.63 ± 1.60	6.70 ± 0.81**	19.33 ± 1.70	6.09 ± 2.27*	94.13 ± 5.15	40.20 ± 5.82**
2	508.5Cer[d18:1C14:1 + H]$^+$	10.36 ± 2.94	8.92 ± 0.64	20.22 ± 5.83	5.19 ± 1.06*	74.64 ± 6.21	32.79 ± 6.58*
3	530.5Cer[d18:1C14:1 + Na]$^+$	7.34 ± 1.06	5.71 ± 1.57	9.29 ± 2.63		49.15 ± 6.89	21.69 ± 6.80**
4	532.5Cer[d18:1C14:0 + Na]$^+$			4.84 ± 0.89		22.82 ± 4.03	15.48 ± 2.55*
5	731.6SM[d18:1C18:0 + H]$^+$	23.35 ± 2.70	75.71 ± 7.98**	56.32 ± 8.07	78.20 ± 9.53**	32.29 ± 1.26	39.37 ± 6.31
6	753.6SM[d18:1C18:0 + Na]$^+$	100.00 ± 0.00	100.00 ± 0.00	100.00 ± 0.00	100.00 ± 0.00	100.00 ± 0.00	100.00 ± 0.00
7	781.6SM[d18:1C20:0 + Na]$^+$	14.37 ± 1.03	12.22 ± 1.95	11.94 ± 1.80	14.35 ± 3.70	16.38 ± 1.95	32.26 ± 3.37*
8	794.6CMH[d18:1C20h:0 + Na]$^+$	3.02 ± 0.39	8.60 ± 4.73			6.58 ± 2.27	11.89 ± 3.16
9	806.7CMH[d18:1C22:0 + Na]$^+$	7.27 ± 0.57	8.58 ± 1.53		8.15 ± 2.26**	15.37 ± 5.17	21.68 ± 5.22
10	810.7CMH[d18:1C24:1 + H]$^+$	3.46 ± 0.38	14.29 ± 2.34**				
11	813.7SM[d18:1C21h:0 + Na]$^+$					11.25 ± 4.11	23.77 ± 1.12*
12	822.7CMH[d18:1C22h:0 + Na]$^+$	17.82 ± 1.09	27.16 ± 5.68*	7.44 ± 1.39	22.60 ± 4.08**	19.78 ± 2.01	38.07 ± 5.51*
13	832.7CMH[d18:1C24:1 + Na]$^+$	13.15 ± 2.20	21.22 ± 5.68	10.43 ± 0.12	14.12 ± 2.45	22.31 ± 2.54	56.51 ± 5.26*
14	834.7CMH[d18:1C24:0 + Na]$^+$	19.22 ± 3.61	17.39 ± 2.11	21.79 ± 4.70	55.68 ± 4.70**	19.61 ± 2.59	55.31 ± 6.63*
15	835.7SM[d18:1C24:1 + Na]$^+$	15.34 ± 2.02	17.75 ± 3.22	15.05 ± 2.56	34.34 ± 3.45**	34.47 ± 6.99	60.45 ± 4.90*
16	836.7CMH[d18:0C24:0 + Na]$^+$	14.39 ± 1.78	29.87 ± 5.74*				
17	848.7CMH[d18:1C24h:0 + Na]$^+$	26.14 ± 2.32	32.76 ± 4.09	12.91 ± 1.16	25.11 ± 4.40*	19.30 ± 1.40	50.81 ± 6.91*
18	850.7CMH[d18:1C24h:0 + Na]$^+$	40.67 ± 3.73	70.24 ± 0.57**	12.60 ± 0.71	51.68 ± 3.60**	37.12 ± 2.89	61.86 ± 5.97*

Cer: ceramide; SM: sphingomyelin; CMH: ceramide-monohexoside, includes glucosylceramide and galactosylceramide; "d" indicates dihydroxy-sphingosine; "h" means there is hydroxyl group in side chain, $n = 7$, compared to control.

* $p < 0.05$.

** $p < 0.01$.

no differential distribution in the different brain regions of normal or PTZ-rats, indicating that they are not modulated by PTZ treatment (Fig. 1).

In contrast, various sphingolipids species did show differential distribution in different brain regions, and PTZ treatment also induced qualitative changes in the sphingolipid profile. An example of differential distribution in normal rats is seen in the greater abundance of ceramides in brain stem than in cortex or hippocampus. Although the implication of this differential distribution is not clear, it is possible that certain functions of the brain stem might be related to the role of ceramide as an important second messenger in many cellular events [4]. But ceramide levels were seen also to respond to PTZ kindling, with significant decreases in the same brain tissue. This observation is in sharp contrast to the report by Guan et al., in which several ceramide molecular species with different acyl compositions are increased during kainate treatment [42]. However, as kainite induces status epilepticus, while PTZ induces absence epilepsy, it is very likely that these two chemicals elicit different effects on sphingolipids metabolism.

There are many "cycles" present in the ceramide biosynthesis pathway. For instance, through the action of SM synthase, ceramide is converted into SM; which, in turn, is hydrolyzed by sphingomyelinase (SMase), regenerating ceramide [4] (Fig. 6). In our experiments, reciprocal changes were observed in ceramide and SM levels, consistent with ceramide cycling. Of course, this reciprocity could result from the activation of SM synthase, or the inhibition of SMase, or both. A similar cycle also relates ceramide to CMH through the actions of CMH synthase (ceramide galactosyltransferase and ceramide glucosyltransferase) and CMH ceramidase (galactosylceramidase and glucosylceramidase). Accordingly, we also observed the increase of CMH concomitant with a decrease in ceramides after PTZ kindling. Whether PTZ could influence the expression/activity of these enzymes in the ceramide biosynthesis pathway is a hypothesis worth testing.

Gangliosides are sialic acid containing glycosphingolipids which also present in the brain. The majority of all mammalian gangliosides are derived from precursor cerebrosides (CMH) [4,44–46] (Fig. 5). Gangliosides have been implicated in brain development, neuritogenesis, memory formation, synaptic transmission and aging [47]. For example, the systemic disruption of the glucosylceramide (GlcCer) synthase gene in mice leads to death during early embryogenesis [48]. A cell-specific disruption in the GlcCer synthase gene also results in major changes in neuronal development [44]. In our experiments, ganglioside levels in the brain tissues could not be assayed due to their relatively low mass signals. However, if ganglioside synthase were inhibited, this could lead to decreased levels of gangliosides in reverse correlation to the accumulation of CMH as we observed. Thus, more sensitive methodology is needed to evaluate the changes in gangliosides by PTZ kindling.

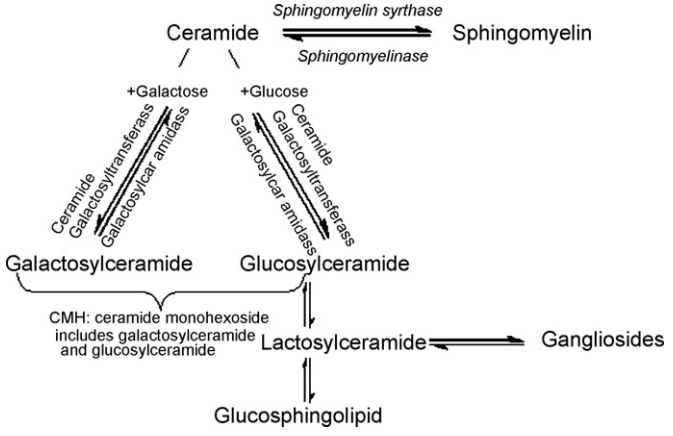

Fig. 6. The metabolic pathway of major sphingolipid species.

In this paper, we analyzed sphingolipids in the brain of normal and PTZ-rats using DE MALDI-TOF-MS. Because of matrix noise in the low mass range of MALDI-TOF-MS spectra, only those relatively abundant sphingolipids could be compared. Yet, in spite of the limitations of the current methodology, this is the first report on sphingolipid profiling in cortex, hippocampus and brain stem from PTZ kindling rats. The changes in brain sphingolipid profiles of PTZ-rats might provide some new clues to understanding the mechanism(s) behind epilepsy.

Acknowledgements

This work was supported in part by grants from the National Natural Science Foundation of China (No. 30600220) and the Startup Funds for Young Scientist from Zhejiang University School of Medicine to X. Ma; NNSF China (Nos. 30471956 and 30771826), New Century Excellent Talent Program of Ministry of Education (NCET-05-0520), Fok Ying Tung Education Foundation (No. 101036), and Zhejiang Provincial Health Bureau (2006QN020) to J. Yang. The authors are grateful to Dr. R. Wohlhueter, recently retired from the Centers for Disease Control and Prevention (CDC, Atlanta, GA), for his editorial assistance.

References

[1] T. Kolter, Angew. Chem. Int. Ed. Engl. 45 (2006) 5910.
[2] M.R. Wenk, Nat. Rev. Drug Discov. 4 (2005) 594.
[3] A.H. Futerman, Y.A. Hannun, EMBO Rep. 5 (2004) 777.
[4] J. Yang, Y. Yu, S. Sun, P.J. Duerksen-Hughes, Cell Biochem. Biophys. 40 (2004) 323.
[5] Y. Kacher, A.H. Futerman, FEBS Lett. 580 (2006) 5510.
[6] T. Kolter, K. Sandhoff, Biochim. Biophys. Acta 1758 (2006) 2057.
[7] W. Zheng, J. Kollmeyer, H. Symolon, A. Momin, E. Munter, E. Wang, S. Kelly, J.C. Allegood, Y. Liu, Q. Peng, H. Ramaraju, M.C. Sullards, M. Cabot, A.H. Merrill Jr., Biochim. Biophys. Acta 1758 (2006) 1864.
[8] X. Han, R.W. Gross, Expert Rev. Proteomics 2 (2005) 253.
[9] M. Lagarde, A. Geloen, M. Record, D. Vance, F. Spener, Biochim. Biophys. Acta 1634 (2003) 61.
[10] R.M. Adibhatla, J.F. Hatcher, R.J. Dempsey, Aaps J. 8 (2006) E314.
[11] X. Han, Front. Biosci. 12 (2007) 2601.
[12] J. Schiller, R. Suss, J. Arnhold, B. Fuchs, J. Lessig, M. Muller, M. Petkovic, H. Spalteholz, O. Zschornig, K. Arnold, Prog. Lipid Res. 43 (2004) 449.
[13] M. Rujoi, R. Estrada, M.C. Yappert, Anal. Chem. 76 (2004) 1657.
[14] R. Estrada, M.C. Yappert, J. Mass Spectrom. 39 (2004) 1531.
[15] B.M. Ham, R.B. Cole, J.T. Jacob, Invest. Ophthalmol. Vis. Sci. 47 (2006) 3330.

[16] S.N. Jackson, H.Y. Wang, A.S. Woods, M. Ugarov, T. Egan, J.A. Schultz, J. Am. Soc. Mass. Spectrom. 16 (2005) 133.
[17] S.N. Jackson, H.Y. Wang, A.S. Woods, J. Am. Soc. Mass. Spectrom. 16 (2005) 2052.
[18] S.N. Jackson, H.Y. Wang, A.S. Woods, Anal. Chem. 77 (2005) 4523.
[19] K. Nakamura, H. Kojima, M. Suzuki, A. Suzuki, Y. Tamai, Eur. J. Biochem. 267 (2000) 5198.
[20] T. Fujiwaki, S. Yamaguchi, M. Tasaka, M. Takayanagi, M. Isobe, T. Taketomi, J. Chromatogr. B Anal. Technol. Biomed. Life Sci. 806 (2004) 47.
[21] T. Fujiwaki, M. Tasaka, N. Takahashi, H. Kobayashi, Y. Murakami, T. Shimada, S. Yamaguchi, J. Chromatogr. B Anal. Technol. Biomed. Life Sci. 832 (2006) 97.
[22] Y. Huang, J. Yang, J. Shen, F.F. Chen, Y. Yu, Biochem. Biophys. Res. Commun. 330 (2005) 430.
[23] Y. Huang, J. Shen, T. Wang, Y.K. Yu, F.F. Chen, J. Yang, Acta Biochim. Biophys. Sin. (Shanghai) 37 (2005) 515.
[24] H.H. Yoo, J. Son, D.H. Kim, J. Chromatogr. B Anal. Technol. Biomed. Life Sci. 843 (2006) 327.
[25] X. Jiang, X. Han, J. Lipid Res. 47 (2006) 1865.
[26] Y. Nagatsuka, H. Tojo, Y. Hirabayashi, Methods Enzymol. 417 (2006) 155.
[27] S. Milne, P. Ivanova, J. Forrester, H. Alex Brown, Methods 39 (2006) 92.
[28] J. Bielawski, Z.M. Szulc, Y.A. Hannun, A. Bielawska, Methods 39 (2006) 82.
[29] X. Han, R.W. Gross, Mass Spectrom. Rev. 24 (2005) 367.
[30] R. Taguchi, T. Houjou, H. Nakanishi, T. Yamazaki, M. Ishida, M. Imagawa, T. Shimizu, J. Chromatogr. B Anal. Technol. Biomed. Life Sci. 823 (2005) 26.
[31] J. Schiller, R. Suss, B. Fuchs, M. Muller, O. Zschornig, K. Arnold, Front. Biosci. 12 (2007) 2568.
[32] K. Morimoto, M. Fahnestock, R.J. Racine, Prog. Neurobiol. 73 (2004) 1.
[33] X.H. Wu, M.P. Ding, Z.B. Zhu-Ge, Y.Y. Zhu, C.L. Jin, Z. Chen, Neurosci. Lett. 400 (2006) 146.
[34] J. Folch, M. Lees, G.H. Sloane Stanley, J. Biol. Chem. 226 (1957) 497.
[35] M. Petkovic, J. Schiller, M. Muller, S. Benard, S. Reichl, K. Arnold, J. Arnhold, Anal. Biochem. 289 (2001) 202.
[36] R. Estrada, M.C. Yappert, J. Mass. Spectrom. 39 (2004) 412.
[37] T. Taketomi, E. Sugiyama, Methods Enzymol. 312 (2000) 80.
[38] C. Bernard, Cell Mol. Life Sci. 62 (2005) 1177.
[39] C.E. Stafstrom, J. Cereb, Blood Flow Metab. 26 (2006) 983.
[40] M.A. Simpson, H. Cross, C. Proukakis, D.A. Priestman, D.C. Neville, G. Reinkensmeier, H. Wang, M. Wiznitzer, K. Gurtz, A. Verganelaki, A. Pryde, M.A. Patton, R.A. Dwek, T.D. Butters, F.M. Platt, A.H. Crosby, Nat. Genet. 36 (2004) 1225.
[41] M. Hermansson, R. Kakela, M. Berghall, A.E. Lehesjoki, P. Somerharju, U. Lahtinen, J. Neurochem. 95 (2005) 609.
[42] X.L. Guan, X. He, W.Y. Ong, W.K. Yeo, G. Shui, M.R. Wenk, Faseb J. 20 (2006) 1152.
[43] Y. Barenholz, T.E. Thompson, Chem. Phys. Lipids 102 (1999) 29.
[44] R. Jennemann, R. Sandhoff, S. Wang, E. Kiss, N. Gretz, C. Zuliani, A. Martin-Villalba, R. Jager, H. Schorle, M. Kenzelmann, M. Bonrouhi, H. Wiegandt, H.J. Grone, Proc. Natl. Acad. Sci. U.S.A. 102 (2005) 12459.
[45] L. Colombaioni, M. Garcia-Gil, Brain Res. Brain Res. Rev. 46 (2004) 328.
[46] G. van Echten-Deckert, T. Herget, Biochim. Biophys. Acta 1758 (2006) 1978.
[47] S. Sonnino, V. Chigorno, Biochim. Biophys. Acta 1469 (2000) 63.
[48] T. Yamashita, R. Wada, T. Sasaki, C. Deng, U. Bierfreund, K. Sandhoff, R.L. Proia, Proc. Natl. Acad. Sci. U.S.A. 96 (1999) 9142.